overlap can be attributed to the difference in hybridization of the metal a_1 orbital: it is a dsp hybrid in the transition metal, with only 5% s character in the octahedral fragment and 4% s character in a square-planar fragment, but an sp hybrid in the main group metal (Al), with 25% s character. The larger s contribution makes the orbital more diffuse for Al (see contour plots in Figure 8), thus avoiding important loss of overlap upon ligand sliding.

Unfortunately, systems with the same ligand for both a transition metal and a main group element have not been studied so far and our comparison cannot be carried on to the experimental data. Let us remark, however, that the calculated barriers for the pdz and naph derivatives are practically identical (Table II), at difference with the results for the analogous derivatives of transition metals. Since the b_2 component of the barrier is negligible for the main group metals, these results confirm our previous assertion that the major difference between both ligands corresponds to their different b_2 repulsions at the bidentate transition state, but not to differences in the loss of a_1 overlap.

Appendix. Computational Details

All calculations were of the Extended Hückel type[26] with modified Wolfsberg-Helmholtz formula.[27] The parameters used were taken from the literature[28] and are collected in Table IV. Calculations were carried out on the following model compounds: fmd^-, fmdH, tzd^-, tzdH, $[CrH_5L]^{5-}$, $[MnH_5L]^{4-}$, $[FeH_5L]^{3-}$, $[FeCp(CO)_2L]^+$, $[PtCl(PH_3)_2(fmd)]$, $[PtCl(PH_3)_2(tzd)]$, $[MCl(PH_3)_2L]^+$ (L = pdz, naph; M = Ni, Pd, Pt). The experimental geometry[5a] was used for fmd and Pt-fmd and kept the same for tzd. Idealized geometries were used for the aromatic ligands pdz and naph, taking all ring distances equal to 1.40 Å, C-H distances of 1.08 Å, and bond angles of 120°. M-N distances were taken as 2.10 Å, a representative value for most of the studied complexes; also frozen representative distances were used for other metal-ligand bonds: M-Cl = 2.20, M-P = 2.20, M-H = 1.75 Å.[5,6,29]

Acknowledgment. The computational part of this work was supported by CAICYT through Grant No. 0657/81. We are indebted to Profs. J. Strähle and T. A. Albright for providing us with their results prior to publication.

(26) Hoffmann, R.; Lipscomb, W. N. *J. Chem. Phys.* **1962**, *36*, 2179, 3469; **1962**, *37*, 2872. Hoffmann, R. *J. Chem. Phys.* **1963**, *39*, 1397.

(27) Ammeter, J.; Bürgi, H.-B.; Thibeault, J.; Hoffmann, R. *J. Am. Chem. Soc.* **1978**, *100*, 3686.

(28) Alvarez, S. *Table of Parameters for Extended Hückel Calculations*; Universitat de Barcelona: Barcelona, 1985.

(29) Teller, R. G.; Bau, R. *Struct. Bond.* **1981**, *44*, 1.

Spin-Orbit Coupling in Biradicals. Ab Initio MCSCF Calculations on Trimethylene and the Methyl-Methyl Radical Pair

Louis Carlacci,[†] Charles Doubleday, Jr.,*[‡] Thomas R. Furlani,[⊥] Harry F. King,*[†] and James W. McIver, Jr.*[†,∥]

Contribution from the Department of Chemistry, State University of New York at Buffalo, Buffalo, New York 14214, Chemistry Department, Columbia University, New York, New York 10027, Calspan Advanced Technology Center, Buffalo, New York 14225, and Department of Chemistry, Canisius College, Buffalo, New York 14208.
Received January 20, 1987

Abstract: Spin-orbit coupling (SOC) constants are computed by ab initio MCSCF (multiconfiguration self-consistent field) theory for the trimethylene biradical, $^{\bullet}CH_2CH_2CH_2^{\bullet}$, and for a pair of interacting methyl radicals as functions of separation and relative orientation of radical centers. The effects of through-bond coupling are analyzed by comparing SOC values for the biradical with those for a radical pair with the same orientation of $^{\bullet}CH_2$ centers. Ab initio results for the radical pair are found to be well-described by the semiempirical formula, SOC = $B|S|\sin\phi$, where ϕ is the acute angle between radical p orbitals, S is the orbital overlap integral, and B = 15 cm^{-1}. Predicted values require correction by a factor of 3.0 or less in the event of strong steric interaction with a radical p orbital. The principal effect of through-bond coupling by a single CH_2 moiety is to increase SOC by another factor of about 2.5. We discuss the implications of these computational results for the interpretation of recently measured rate constants for intersystem crossing in a 1,3- and a 1,4-biradical system. We conclude that the slower rate in the 1,3-biradical is due to the Boltzmann factor associated with the activation energy required to reach the singlet-triplet crossing.

A major challenge in the chemistry of organic biradicals and radical pairs is the problem of treating intersystem crossing (ISC) between singlet and triplet states. The problem is important because biradicals generated from triplet precursors must first undergo ISC before products can be formed. Thus, ISC influences both the rate of product formation[1] and the product ratio.[2] Scheme I presents a general kinetic model that has proved useful for interpreting experimental results. Three categories of kinetic processes are important: (1) ISC; (2) chain dynamics in the case of biradicals or diffusive displacements in the case of radical pairs in solution; (3) the product-forming step, typically a process on the singlet surface.

[†] State University of New York at Buffalo.
[‡] Columbia University.
[⊥] Calspan Advanced Technology Center.
[∥] Canisius College.

(1) (a) Zimmt, M. B.; Doubleday, C. Jr.; Turro, N. J. *J. Am. Chem. Soc.* **1986**, *108*, 3618-3620. (b) Caldwell, R. A. *Pure Appl. Chem.* **1984**, *56*, 1167-1177. (c) Scaiano, J. C. *Acc. Chem. Res.* **1982**, *15*, 252-258. (d) Closs, G. L.; Miller, R. J.; Redwine, O. D. *Ibid.* **1985**, *18*, 196-202.

(2) (a) Doubleday, C., Jr. *Chem. Phys. Lett.* **1979**, *64*, 67-70. (b) Doubleday, C., Jr. *Chem. Phys. Lett.* **1981**, *79*, 375-380. (c) Caldwell, R. A.; Creed, D. *J. Phys. Chem.* **1978**, *82*, 2644-2652. (d) Scaiano, J. C.; Lee, C. W. B.; Chow, Y. L.; Marciniak, B. *Ibid.* **1982**, *86*, 2452-2455. (e) Scaiano, J. C. *Tetrahedron* **1982**, *38*, 819-824.

0002-7863/87/1509-5323$01.50/0

Scheme I

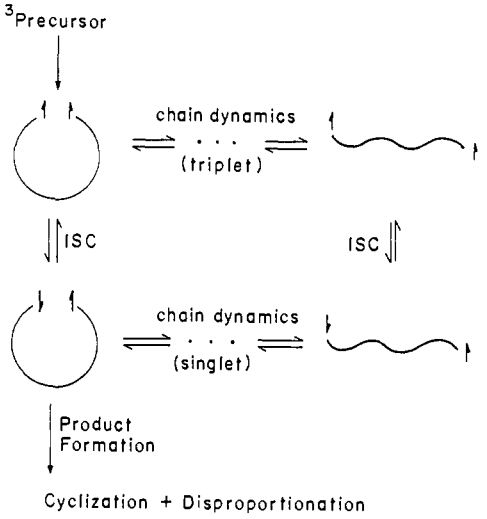

This paper is concerned with the ISC step. Usually,[1] but not always,[1a,3] this is the rate-determining step for product formation in biradicals, and recently one of us has elaborated the conditions under which either ISC or chain dynamics can be rate-determining.[1a] Two different mechanisms give rise to ISC, namely, electron–nuclear hyperfine coupling (HFC) and spin–orbit coupling (SOC). The HFC mechanism, as the source of CIDNP[4a] and magnetic isotope effects,[4b,c] has been extensively studied. SOC, on the other hand, has only recently been positively identified as the *primary* ISC mechanism in biradicals.[1d,5] In a few cases the individual contributions of SOC and HFC to the total ISC have been measured.[5b,c] Previous results by Caldwell[1b] and Scaiano[6] suggested that SOC is a significant ISC mechanism. HFC and SOC and their geometry dependences and their roles in controlling CIDNP processes have been discussed by de Kanter and Kaptein.[7]

Salem and Rowland presented the first qualitative theoretical discussion of SOC specifically applied to biradicals.[8] This pioneering study identified three important features: SOC is proportional to the zwitterionic character of the singlet state; it is proportional to the degree to which the orientations of the two singly occupied atomic orbitals are perpendicular; and it decreases sharply as the distance, R, between radical centers increases.

$$\text{SOC } \alpha \text{ ionic character} \tag{1a}$$

$$\text{SOC } \alpha \text{ orbital perpendicularity} \tag{1b}$$

$$\text{SOC decreases as } R \text{ increases} \tag{1c}$$

Salem and Rowland also noted the qualitative importance of overlap in influencing SOC. Shaik and Epiotis[9] discuss the relationship of SOC to the symmetries of nuclear motion in biradicals, and Turro and Devaquet[10] discuss several qualitative aspects of SOC in connection with thermal generation of triplet states from dioxetanes. The first ab initio calculations of SOC in biradicals were recently carried out by two of us[11] who computed SOC constants for trimethylene using the full Breit–Pauli spin–orbit Hamiltonian[12] and multiconfiguration self-consistent-field (MCSCF) wave functions.[13] The results were consistent with the qualitative predictions of Salem and Rowland.[8]

The purpose of the present paper is to examine computationally the geometry dependence of the SOC constant in biradicals with use of the ab initio procedure previously described.[11] To this end, the SOC constant for a pair of methyl radicals has been computed at a large number of relative orientations and intercarbon distances. It is demonstrated that the principal features of the geometry dependence of SOC are reproduced by a semiempirical formula that incorporates the factors listed above in eq 1. The SOC constant in the trimethylene biradical is discussed in terms of through-space and through-bond contributions. We define the through-space coupling contribution to be SOC for a methyl radical pair whose geometry resembles that of the terminal CH_2 groups of the biradical.

In the next section we briefly review the general theory and present the semiempirical formula for the geometry dependence of the SOC constant. This section is followed by a description of the coordinate systems used for the methyl–methyl pair and trimethylene. Computational results are then reported as contour diagrams of the SOC constants obtained by the ab initio calculations and by the semiempirical formula. Finally, in the discussion section, we comment on the effect of through-bond coupling, the utility of the semiempirical formula, and implications of the theoretical results for the interpretation of recently observed ISC rate constants.

Theory

As discussed previously,[11] the Breit–Pauli spin–orbit Hamiltonian[12] is written as

$$\hat{H}_{so} = \frac{e^2\hbar}{2m^2c^2}\{\sum_{i,k} Z_k\, r_{ik}^{-3}[(\mathrm{r}_i - \mathrm{r}_k) \times \hat{\mathbf{p}}_i]\cdot\hat{\mathbf{s}}_i - \sum_{i\neq j} r_{ij}^{-3}[(\mathrm{r}_i - \mathrm{r}_j) \times \hat{\mathbf{p}}_i]\cdot[\hat{\mathbf{s}}_i + 2\hat{\mathbf{s}}_j]\} \tag{2}$$

where $\hat{\mathbf{p}}_i$ is the momentum operator and $\hat{\mathbf{s}}_i$ the dimensionless spin operator of electron i, and Z_k is the atomic number of the kth nucleus. The spin–orbit coupling constant is the matrix element that expresses the coupling of singlet and triplet states by this operator.

$$\mathrm{SOC}(M_s) = \langle {}^1\psi|\hat{H}_{so}|{}^3\psi(M_s)\rangle \tag{3}$$

Here ${}^1\psi$ is the many-body, singlet-state wave function, and ${}^3\psi(M_s)$ is the M_s component of the triplet wave function. The $M_s = \pm 1$ components are complex conjugates of one another, so that the $M_s = \pm 1$ coupling constants have the same absolute magnitude. For a typical experiment carried out in the earth's magnetic field, the three triplet sublevels are effectively degenerate. Thus a reasonable measure of SOC-induced singlet–triplet interaction is the root-mean-square coupling constant.

$$\mathrm{SOC}_{rms} = [\sum_{M_s}|\mathrm{SOC}(M_s)|^2]^{1/2} \tag{4}$$

In this paper a value for SOC always implies SOC_{rms}. Individual contributions of 1-electron and 2-electron, real and imaginary terms of each component were previously reported for trimethylene.[11]

Small CAS–MCSCF (complete active space multiconfiguration self-consistent-field) wave functions[13] were employed in these calculations. The orbital space in a CAS–MCSCF calculation is partitioned into three subspaces: N_c, doubly occupied core

(3) Lee, K. W.; Hanckel, J. M.; Brown, T. J. *J. Am. Chem. Soc.* **1986**, *108*, 2266–2273.
(4) (a) Kaptein, R. *Adv. Free Radical Chem.* **1975**, *5*, 319–380. (b) Turro, N. J.; Kraeutler, B. In *Isotopic Effects*, Vol. 6 of *Isotopes in Organic Chemistry*; Buncel, E., Lee, C. C., Eds.; Elsevier: Amsterdam, 1984; p 107. (c) Gould, I. R.; Turro, N. J.; Zimmt, M. B. *Adv. Phys. Org. Chem.* **1984**, *20*, 1–53.
(5) (a) Zimmt, M. B.; Doubleday, C., Jr.; Gould, I.; Turro, N. J. *J. Am. Chem. Soc.* **1985**, *107*, 6724–6726. (b) Zimmt, M. B.; Doubleday, C., Jr.; Turro, N. J. *Ibid.* **1985**, *107*, 6726–6727. (c) Closs, G. L.; Redwine, O. D. *Ibid.* **1985**, *107*, 4543–4344, 6131–6133.
(6) (a) Weir, D.; Scaiano, J. C. *Chem. Pys. Lett.* **1985**, *118*, 526–529. (b) Johnson, L.; Scaiano, J. C.; Sheppard, J. *Chem. Phys. Lett.* **1986**, *124*, 493–496. (c) Barton, D. H. R.; Charpiot, B.; Ingold, K. U.; Johnston, L. J.; Motherwell, W. B.; Scaiano, J. C.; Stanforth, S. *J. Am. Chem. Soc.* **1985**, *107*, 3607–3611.
(7) de Kanter, F. J. J.; Kaptein, R. *J. Am. Chem. Soc.* **1982**, *104*, 4759–4766.
(8) Salem, L.; Rowland, C. *Angew. Chem., Int. Ed. Engl.* **1972**, *11*, 92–111.
(9) (a) Shaik, S. S.; Epiotis, N. D. *J. Am. Chem. Soc.* **1978**, *100*, 18–29. (b) Shaik, S. S. *Ibid.* **1979**, *101*, 2736–2736, 3184–3196.
(10) Turro, N. J.; Davaquet, A. *J. Am. Chem. Soc.* **1975**, *97*, 3859–3862.
(11) Furlani, R.; King, H. F. *J. Chem. Phys.* **1985**, *82*, 5577–5583.
(12) Langhoff, S. R. In *Applications of Electronic Structure Theory*, Vol. 4 of *Modern Theoretical Chemistry*; Schaefer, H. F. III, Ed.; Plenum: New York, 1977; p 384.
(13) (a) Siegbahn, P. E. M.; Almlöf, J.; Heiberg, A.; Roos, B. O. *J. Chem. Phys.* **1981**, *74*, 7384–7396. (b) Roos, B. O.; Taylor, P. R.; Siegbahn, P. E. M. *Chem. Phys.* **1980**, *48*, 157–173.

molecular orbitals; N_a, variably occupied active orbitals; and N_v, unoccupied virtual orbitals. The CAS–MCSCF wave function is an optimized linear combination of configuration state functions (CSFs).

$$^{2S'+1}\psi(M_s) = \sum_i C_i \mathrm{CSF}_i(S',M_s) \quad (5)$$

Each CSF is itself a spin-adapted linear combination of Slater determinants. Spin-adapted implies that each CSF is an eigenfunction of $\hat{S}^2$ and $\hat{M}_s$ with eigenvalues $S'(S'+1)$ and M_s, respectively. The summation in eq 5 is complete in the sense that it includes all CSFs consistent with the given values of N_a, S', and M_s. Such a calculation with N_e electrons and N_a spatial orbitals in the active space is referred to as an N_e-in-N_a CAS. Calculations reported in this paper employ simple 2-in-2 CAS wave functions. The singlet state function consists of 3 CSFs. The triplet state wave function consists of a single CSF, in this case equivalent to an RHF triplet function. It is a general feature of the CAS formalism that there are more low-spin than high-spin CSF. This is necessary in order to achieve an even-handed representation of the two different spin states, and it is a common aspect of accurate ab initio computations such as the definitive study of spin–orbit coupling in methylene by Langhoff et al.[14] In the usual MCSCF procedure the configuration interaction coefficients, C_i, and the molecular orbitals defining the CSF_i are all simultaneously varied to minimize the state energy.[13] The resulting occupied singlet spatial MOs rarely span the same orbital space as do those for the triplet state. To simplify the computation, we constrain the singlet core orbitals to be identical with those for the triplet but allow the active orbitals to vary freely. Unless stated otherwise, all orbitals are expanded by using a 3-21G split-valence basis set.[15] We regard this 2-in-2, frozen-core procedure as being the minimal theoretical level for spin–orbit calculations. The wave functions have sufficient flexibility to describe essential features of the electronic structure such as freedom for singlet and triplet active orbitals (the radical site p orbitals) to respond each in its own way to geometrical changes and variational freedom to determine the extent of partial pairing of the "unpaired" electrons in the singlet state. This last feature is required for an unbiased measure of ionic character. In this respect, the restricted or unrestricted Hartree–Fock formalism is unsatisfactory for this application.

It would be very useful to have a simple approximate formula for estimating the geometry dependence of the SOC constant in more complicated biradicals. Such a formula would be used to predict optimal orientations for ISC and to rationalize experimental observations. We suggest the following:

$$\mathrm{SOC} = B(R)|S| \sin\phi \quad (6)$$

Here ϕ is the acute angle between the p atomic orbitals containing the unpaired electrons, S is the overlap integral for these orbitals, and B is a slowly varying function of R independent of angular orientation. Consider a unit vector to be directed along the axis of the radical site p orbital. By definition, the dot product of two such unit vectors is the cosine of ϕ. This angle is zero for collinear p orbitals as well as for parallel p orbitals as in a π bond. For simplicity, let the radical site p orbital be a Slater 2p function perpendicular to the terminal methylene plane. The integral in eq 6 is then a weighted sum of two overlap integrals give by

$$S_\pi(\rho) = (1 + \rho + 2\rho^2/5 + \rho^3/15)e^{-\rho} \quad (7a)$$

and

$$S_\sigma(\rho) = (-1 - \rho - \rho^2/5 + 2\rho^3/15 + \rho^4/15)e^{-\rho} \quad (7b)$$

where $\rho = 3.0708R$ when R is expressed in angstrom units corresponding to the Slater rules value for carbon, namely, $\zeta_{2p} = 1.625$ bohr^{-1}. The overlap integral in eq 6 introduces an approximately exponential dependence of SOC on the separation of the radical centers and expresses the relationship between SOC and ionic character in accord with an earlier analysis[16] that showed that S is rougly proportional to percent ionic character under conditions thought to be satisfied in polymethylenes. Thus eq 6 incorporates the principal factors listed in eq 1 above. Qualitative arguments connecting eq 1 and 2 have been advanced by Salem and Rowland[8] and more recently by Shaik and Epiotis,[9] Turro and Davaquet,[10] and de Kanter and Kaptein.[7] The essential physical requirement for two functions to be coupled by the $\hat{H}_{so}$ operator is that in going from one to the other a change in electron spin angular momentum must be accompanied by an appropriate change in orbital angular momentum. In effect, parallel p orbitals have the same orbital angular momentum, and SOC is zero if they constitute the entire active orbital space. This leads to the sin ϕ factor in eq 6. Similar arguments apply to the ionic character and hence to the orbital overlap condition.[8-10,16] In view of the various approximations and assumptions involved, we make no attempt to further defend the arguments that led us to eq 6 but simply propose it as being a reasonable hypothesis whose validity is to be established by comparing its predictions with those of a more rigorous theory.

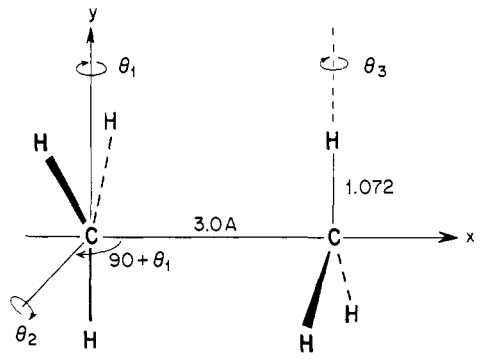

Figure 1. Definition of rotation angles $(\theta_1,\theta_2,\theta_3)$ for a pair of methyl radicals. Individual methyls are planar. The face-to-face orientation shown above is the reference orientation, (0,0,0). The general orientation, $(\theta_1,\theta_2,\theta_3)$, is obtained from the refereence by a rotation of the first methyl θ_1 about the y axis followed by a rotation θ_2 about the body-fixed $\bar{z}$ axis and rotation of the second methyl θ_3 about an axis passing through its center parallel to y.

Coordinates

Figure 1 shows a pair of methyl radicals, each with D_{3h} symmetry, in the staggered face-to-face orientation. The first radical, at the origin of the Cartesian frame, lies in the yz plane with its p orbital along the x axis and a C–H bond along the negative y axis. The second radical is displaced a distance R along the positive x axis and rotated half a turn about that axis. Consider rigid rotational displacements of the methyl groups from this reference orientation. Angles θ_1, θ_2, and θ_3 refer to three of the five possible degrees of rotational freedom. Let the first radical be rotated through an angle θ_1 about the y axis followed by a rotation θ_2 about the body-fixed $\bar{z}$ axis. Axes z and $\bar{z}$ coincide in the reference orientation. In general, $\bar{z}$ lies in the xz plane at an angle $\theta_1 + (\pi/2)$ with respect to x. The resulting orientation can be achieved, alternatively, by a rotation θ_2 about the z axis followed by a rotation θ_1 about the y axis. The second methyl is rotated θ_3 about an axis passing through its center parallel to the y axis. A positive rotation is defined to be one that appears counterclockwise when viewed from the origin looking out along the positive rotation axis. The following orientations are symmetrically equivalent:

$$(\theta_1,\theta_2,\theta_3) \leftrightarrow (\theta_1,\theta_2,\theta_3+\pi) \leftrightarrow (-\theta_1,\theta_2,-\theta_3) \leftrightarrow (\theta_1+\pi,-\theta_2,\theta_3) \quad (8)$$

The angle ϕ between p orbitals is related to θ_1, θ_2, and θ_3 by

$$\cos\phi = |\cos\theta_2 \cos(\theta_1 - \theta_3)| \quad (9)$$

We consider a second set of methyl–methyl pair orientations chosen to resemble the terminal methylene groups in the tri-

(14) McKellar, A. R. W.; Bunker, P. R.; Sears, T. J.; Evenson, K. M.; Saykally, R. J.; Langhoff, S. R. *J. Chem. Phys.* **1983**, *79*, 5251–5264.
(15) Binkley, J. S., Jr.; Pople, J. A.; Hehre, W. J. *J. Am. Chem. Soc.* **1980**, *102*, 939–947.
(16) Doubleday, C., Jr.; McIver, J. W., Jr.; Page, M. *J. Am. Chem. Soc.* **1982**, *104*, 6533–6542.

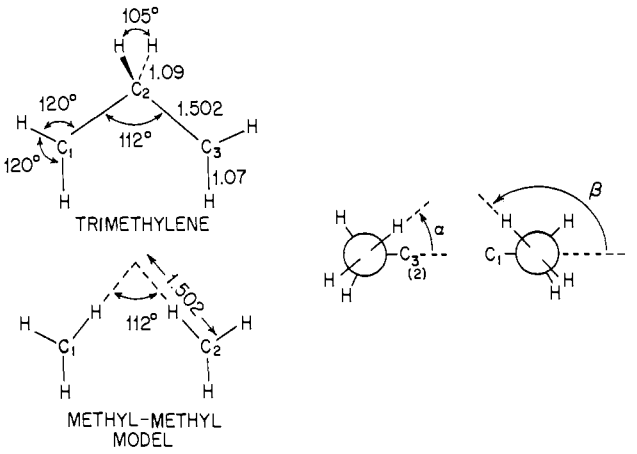

Figure 2. Definitions of α and β rotation angles for trimethylene and the methyl–methyl model of trimethylene. The geometric parameters are the same as in ref 11 and 16.

methylene biradical. Members of this set are described by angles α and β.[17] The reference geometry of the trimethylene biradical and the corresponding model methyl–methyl radical pair and the meaning of the α and β rotation angles are described in Figure 2. Note that the terminal methylene groups in the model can be superimposed on those in the biradical. The reference orientation with C_{2v} molecular symmetry corresponds to $\alpha = \beta = 0$. These angles measure internal rotation about the C–C bonds in the biradical or about the corresponding C–H bonds in the model. Conrotatory displacements, those which reduce the symmetry from C_{2v} to C_2, correspond to $\alpha = \beta$. Disrotatory displacements, those which reduce the symmetry from C_{2v} to C_s, corresponds to $\alpha = -\beta$. The angle ϕ between p orbitals is related to these internal rotation angles by

$$\cos \phi = |\cos \alpha \cos \beta + \cos (112°) \sin \alpha \sin \beta| \quad (10)$$

Our purpose in studying these particular orientations of the methyl radical pair is to examine the separate contributions of through-bond and through-space interactions to SOC in trimethylene. Replacing the central CH_2 moiety in trimethylene by a pair of hydrogen atoms removes the connecting covalent carbon–carbon bonds while preserving the spatial arrangement of the radical centers. Thus the spin–orbit coupling in the radical pair model is, by definition, due to a through-space interaction. The added hydrogens are, however, severely interpenetrating. The H–H separation is only 0.72 Å, very nearly that in the hydrogen molecule. In going from trimethylene to the radical pair model, covalent bonding has been replaced, unavoidably, by steric repulsion.

Computational Results

Ab initio results for the methyl–methyl radical pair, the trimethylene biradical, and the radial pair model of trimethylene are displayed as SOC contour maps in Figure 3–6. Grids of SOC values were generated for the radical pair at a separation of R = 3.0 Å by varying θ_1 and θ_3 over their entire range in increments of 45° for fixed values of θ_2. Interpolation between grid points was accomplished by using cubic spline fits, and a few additional ab initio points were generated where needed to produce the contour maps. Results for $\theta_2 = 0$ and 45° are shown in Figures 3 and 4, respectively. These maps are simply repeated when θ_1 or θ_3 is extended beyond the range shown, in accord with (8). Figure 3 demonstrates that spin–orbit interaction is weak unless orbital overlap and orbital perpendicularity are both favorable. Neither factor by itself is sufficient. Note, for example, that SOC is zero in the center of the figure, i.e., in the face-to-face orientation, $(\theta_1,\theta_2,\theta_3) = (0,0,0)$, where the p orbitals achieve maximum overlap but are colinear, and it is small, SOC(90°,0,0) = 0.012

(17) The two sets are not disjoint. The (58.866°, 31.134°) orientation is equivalent to (16.806°, −60°, 73.194°).

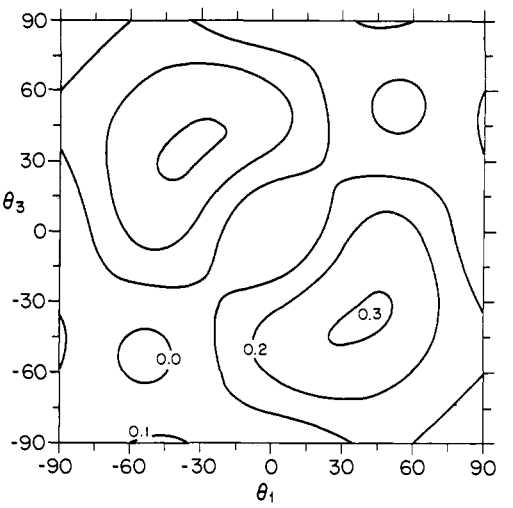

Figure 3. SOC(θ_1,0°,θ_3). Ab initio root-mean-square spin–orbit coupling constant for the methyl–methyl radical pair at a carbon–carbon distance of 3.0 Å. Coordinates are those shown in Figure 1. Contour lines are plotted at intervals of 0.1 cm^{-1}.

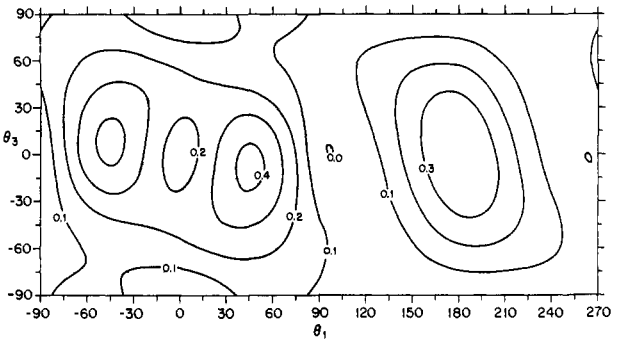

Figure 4. SOC(θ_1,45°,θ_3). See caption for Figure 3.

cm^{-1}, where the p orbitals are perpendicular but have zero overlap. The maximum in Figure 3, SOC(35°,0,−35°) = 0.35 cm^{-1}, occurs where both factors are favorable. The results displayed in Figure 4 provide further support for this conclusion, but they also demonstrate the shortcomings of an attempt to describe spin–orbit interaction solely in terms of the orientation of the radical p orbitals, each assumed to be perpendicular to its methyl plane. For example, orientations (45°,0,0), (0,45°,0), and 0,−45°,0) have significantly different SOC values, namely, 0.241, 0.158, and 0.391 cm^{-1}, respectively, but they are indistinguishable if one considers only the radical p orbitals (one p orbital directed along the carbon–carbon line of centers, the other pointing off at a 45° angle). The relevant geometrical feature that distinguishes these three orientations appears to involve a hydrogen atom bonded to one center intruding into the region normally occupied by the p orbital of the other radical. The broad region of high SOC values on the right-hand side of Figure 4 and the pair of less prominent peaks to its left correspond to each of the three hydrogens entering, in turn, the region between the two carbon atoms as the first radical rotates about the y axis. This feature becomes more pronounced as θ_2 increases. The greatest spin–orbit coupling computed for a methyl radical pair with separation R = 3.0 Å, SOC(0,−60°,0) = 0.437 cm^{-1}, occurs in the geometry shown below, which apparently represents a compromise along the three factors discussed.

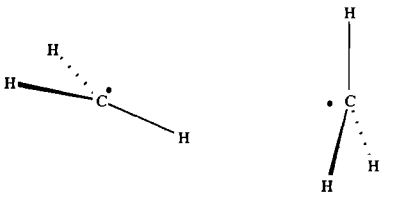

(0°,-60°,0°)

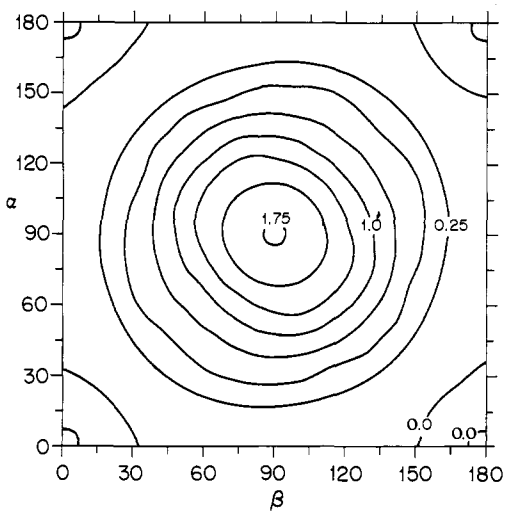

Figure 5. SOC(α,β). Ab initio root-mean-square spin–orbit coupling constant for the trimethylene biradical at a carbon–carbon distance of 2.490 Å. Coordinates are those shown in Figure 2. Contour lines are plotted at intervals of 0.25 cm^{-1}.

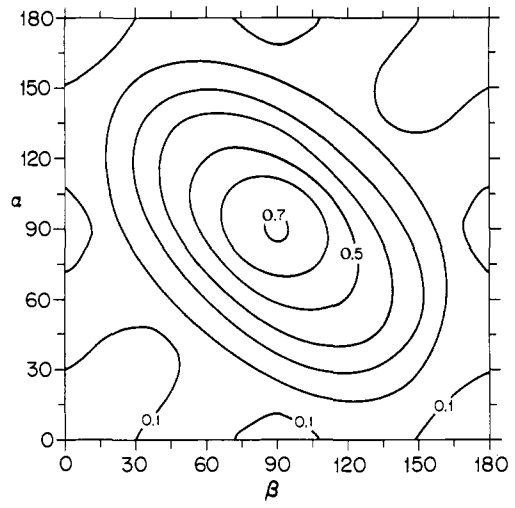

Figure 6. SOC(α,β). Ab initio root-mean-square spin–orbit coupling constant for the methyl–methyl radical pair model of trimethylene at a carbon–carbon distance of 2.490 Å. Coordinates are those shown in Figure 2. Contour lines are plotted at intervals of 0.1 cm^{-1}.

Figure 5 is an improved version of an ab initio contour map presented[18] in ref 11 showing spin–orbit coupling, SOC(α,β), in the trimethylene biradical as a function of internal rotation angles. Note that the corners of the figure are circumscribed by nodal contour lines. The (90°,90°) orientation, in the center of the figure, corresponds to the radical p orbitals having been rotated into the carbon atom plane where they achieve maximum overlap and maximum perpendicularity (68°). The contour map is dominated by a single broad peak with its maximum at this orientation. Conrotatory displacements from (90°,90°) decrease SOC somewhat faster than do disrotatory displacements, giving a slightly elliptical shape to the contour lines in the central area of the map. Spin–orbit coupling is weak for geometries corresponding to the edges of Figure 5. This is attributed to a combination of unfavorable orbital alignment and poor overlap. For example, in the lower left-hand corner of the figure the p orbitals are parallel (as in a π bond) and coupling is negligible, SOC(0,0) = 0.004 cm^{-1}. At the midpoint of the bottom edge of the figure p orbital overlap is zero and coupling is weak, SOC(0,90°) = 0.023 cm^{-1}. The ab initio contour map for the methyl radical pair model of trimethylene is shown in Figure 6. It too exhibits a prominent peak centered on the (90°,90°) orientation, falling off to low SOC values in the corners of the figure, but the maximum coupling for the radical pair model is only 0.705 cm^{-1} compared with 1.760 cm^{-1} for trimethylene itself. A rough approximation to the trimethylene map is obtained by scaling up that for the model by a factor of 2.5. There are, however, discernable differences between the scaled up SOC map for the model and that for trimethylene. In particular, the contour lines in the center of Figure 6 are more elliptical than those in Figure 5, and the nodal lines are absent.

(18) Table IV in ref 11 contains an error. The individual one- and two-particle contributions to SOC(35°, 35°) for $M_s = 0$ are correct, but their sum is 0.201 not 0.041 as reported. Thus SOC_{rms}(35°, 35°) = 0.211 cm^{-1} not 0.077 cm^{-1} as reported. The contour map and fitting constants given on p 5582 of ref 11 were generated with use of the spurious value.

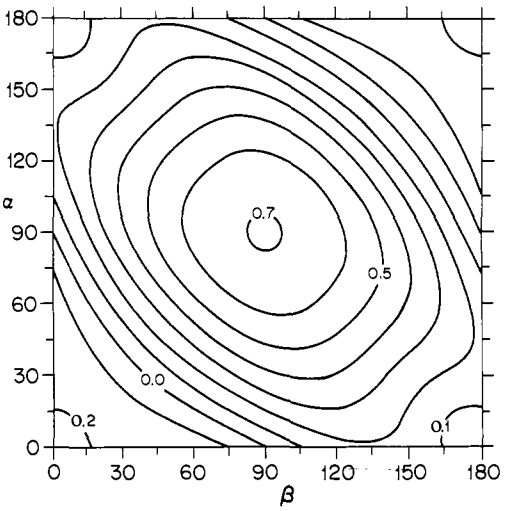

Figure 7. SOC(α,β). Semiempirical formula, eq 6, with R = 2.490 Å and B = 12.64 cm^{-1}. Contour lines are plotted at intervals of 0.1 cm^{-1}. This is the semiempirical version of Figure 6.

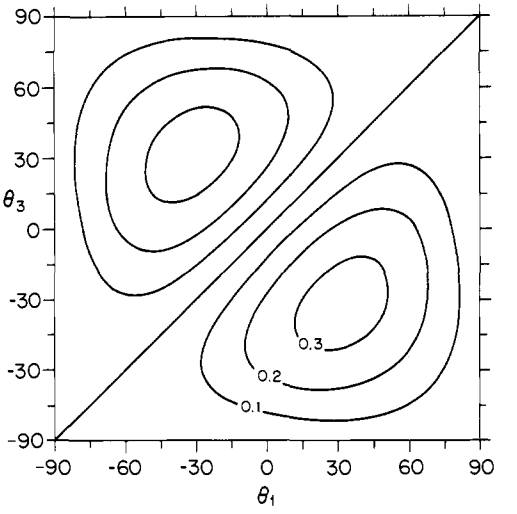

Figure 8. SOC(θ_1,0°,θ_3). Semiempirical formula, eq 6, with R = 3 Å and B = 8.92 cm^{-1}. Contour lines are plotted at intervals of 0.1 cm^{-1}. This is the semiempirical version of Figure 3.

In Figure 7 is shown a contour map of SOC(α,β) generated by using eq 6 with R = 2.49 Å, $B(R)$ = 12.64 cm^{-1}, and the overlap integral given by

$$S = S_\pi \cos\alpha \cos\beta - \tfrac{1}{2}[(S_\sigma + S_\pi) + (S_\sigma - S_\pi)\cos(112°)] \sin\alpha \sin\beta$$
$$= 0.2952 \cos\alpha \cos\beta - 0.06018 \sin\alpha \sin\beta \quad (11)$$

The B factor has been chosen so that SOC(90°,90°) = 0.705 cm^{-1} in agreement with the ab initio result for the methyl radical pair model. The corners of Figure 7 represent points where spin–orbit interaction is predicted to vanish due to the sin ϕ factor. The nodel line passing through (0°,90°) and (35°,35°) is the locus of points where eq 6 vanishes due to zero orbital overlap. Note that the

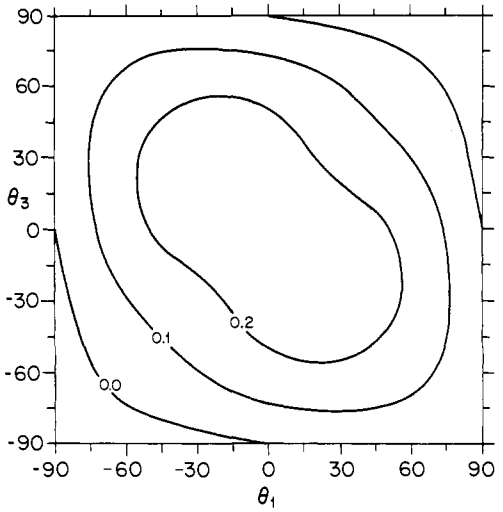

Figure 9. SOC(θ_1,45°,θ_3). This map is simply repeated when θ_1 is extended beyond 90°. See caption for Figure 8. This is the semiempirical version of Figure 4.

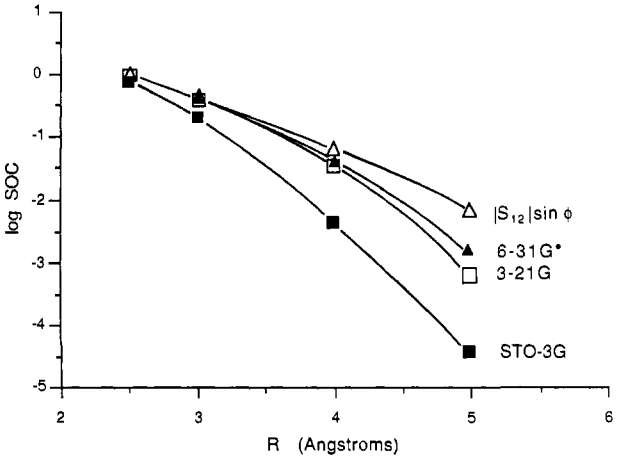

Figure 10. SOC(0°,-45,0°). Ab initio coupling constants computed by using three different Gaussian basis sets for the methyl–methyl radical pair as a function of carbon–carbon distance. Also shown is the semiempirical formula evaluated with fixed B = 15 cm^{-1}.

contour lines in the central region of Figure 7 are more elliptical than those in Figure 6 and considerably more so than those in Figure 5. This elliptical shape is associated with the fact that orbital overlap changes sign for conrotatory but not for disrotatory internal rotation, with the result that nodal lines occur only in the lower left and upper right areas of Figure 1. In other aspects, the semiempirical formula reproduces the qualitative features of the ab initio calculation for the methyl radical pair. In another test of the semiempirical formula, eq 6 was evaluated as a function of θ_1 and θ_3 for R = 3 Å and θ_2 = 0° with use of $B(R)$ = 8.92 cm^{-1}. The results, plotted in Figure 8, compare well with the ab initio results given in Figure 3. The semiempirical formula fails, however, to describe the previously discussed enhancement of SOC by intrusion of a C–H bond. For example, the semiempirical representation of SOC(θ_1,45°,θ_3) (Figure 9) lacks the three peaks exhibited in the ab initio map (Figure 4). Finally, Figure 10 provides information concerning basis set effects and the dependence of spin–orbit coupling on R. Shown in the figure is the logarithm of SOC(0,-45°,0) computed for a pair of methyl radicals at distances varying from 2.5 to 5 Å with use of three different Gaussian orbital basis sets: a minimal basis, a split-valence basis, and a split-valence set with d-type polarization functions on carbons. The computed spin–orbit coupling constant is quite sensitive to the quality of the basis set, particularly when the radical centers are widely separated. Although the split-valence sets do not differ remarkably from a minimal basis in the exponents of their most diffuse primitive Gaussian functions, they appear to provide a much improved description of long-range through-space coupling. Also shown in Figure 10 is the semiempirical formula evaluated for fixed $B(R)$ = 15 cm^{-1}. In this case, SOC is simply proportional to S_σ. Because the empirical formula is based on an assumed exponential orbital tail, it constitutes our current best guess as to how to extrapolate computed coupling constants to large R values.

Discussion

It is expected that through-bond coupling (TBC) is rapidly attenuated with increasing number of bonds connecting the radical centers. A comparison of Figure 5 with Figure 6 reaveals the effects of TBC for a single connecting CH_2 moiety. The SOC(α,β) function resulting from both through-space and through-bond interactions (Figure 5) is approximately a scaled-up version of that due to through-space interactions alons (Figure 6). This suggests that TBC is better thought of as a multiplicative rather than an additive correction to the through-space SOC(α,β) function. Although eq 2 and 3 provide a fundamentally sound basis for numerical computation of spin–orbit coupling, further analysis is required for the interpretation of numerical results. We are not aware of such an analysis of SOC which favors an additive or multiplicative or any other form of TBC. The multiplicative view has in its favor the simplifying feature that one need ascribe only weak geometry dependence to the TBC correction factor. To a first approximation, the results presented in Figures 5 and 6 correspond to a constant TBC factor for trimethylene equal to 2.5, independent of twist angles α and β. This does not imply that TBC is independent of twist angles but rather that through-space and through-bond coupling both vary with α and β in much the same way. Since the trimethylene-like radical pair is extremely crowded, the "through-space interaction" is perhaps more properly described in the words of a referee as a "through-antibond interaction". In any case, Figures 5–7 demonstrate that bonding, antibonding, and nonbonding (through-space) interactions all vary in much the same way when the polymethylene chain is twisted. If one accepts R = 3 Å as being sufficiently remote to correspond to a true through-space interaction, and if one accepts that eq 6 provides an adequate representation of SOC at 3 Å, then one is inclined to accept eq 6 as a general representation of through-space coupling. Note that the through-antibond interaction displaced in Figure 6 is not significantly different from the through-space interaction displayed in Figure 7. Closer inspection of Figures 5 and 6 reveals that in the course of a disrotatory motion, along the principal diagonal in the figure, the effect of TBC is to first decrease then increase the spin–orbit interaction. It is as though through-bond and through-space interactions partially cancel one another when the radical p orbitals are in a π-type conformation. Perhaps this is somehow related to the fact that the connecting CH_2 group in trimethylene has a doubly occupied orbital with π-type symmetry in the C_{2v} geometry. In any case, the observed cancelation occurs for geometries in which SOC is small for both the biradical and the radical pair. It is likely that the observed factor of 2.5 represents an upper limit on the magnitude of the TBC effect for aliphatic biradicals.

The proposed semiempirical spin–orbit interaction expression, eq 6, incorporates the principal factors listed in eq 1 and is in substantial agreement with all of our ab initio results. In fact, we are astounded by its success. The rationale behind eq 6 takes no account of two-electron terms in the Breit–Pauli spin–orbit Hamiltonian even though their contribution to SOC is far from negligible. In trimethylene the major effect of the two-electron operator is to partially screen the carbon atom from the unpaired electrons and so reduce SOC by a factor of about 2.0, but there exist geometries, e.g., (0,0), for which the cancellation of one- and two-electron terms is considerably greater than this.[11] Nonetheless, we conclude that large ϕ and S is a necessary condition for large spin–orbit interaction in methyl radical pairs. No geometrical conformation with large ab initio SOC value was encounted that had nearly parallel radical p orbitals or small p orbital overlap. We did encounter conformations in which spin–orbit coupling

appeared to be enhanced by intrusion of a C–H moiety into the region normally occupied by a radical p orbital, but even in these cases ab initio SOC values are very small when predicted by eq 6 to be so. A comparison of Figure 4 with Figure 9 suggest that the intrusion effect can increase SOC by as much as a factor of 3. A better understanding of this phenomenon requires further analysis of the molecular spin density.[19] Perhaps the Pauli exclusion principle requires a local distortion of the radical p orbital in the vicinity of the intruder orbital and so introduces new localized angular momentum components. In any case the effect is expected to be associated with steric repulsion and thus not to be of great practical importance except under crowded conditions. When computing contour maps of the semiempirical function (Figures 7–9), we let the $B(R)$ factor decrease slowly with increasing separation between radical centers, namely, $B(2.49)$ = 12.94 cm^{-1} and $B(3.0)$ = 8.92 cm^{-1}. This produced the best fit to the available ab initio results, but we hesitate to attach too much significance to this R dependence. We anticipate that use of the small 3-21G basis set[15] leads to underestimation of the spin–orbit interaction and that the basis set error becomes more severe with increasing separation between radical centers. In fact, we tentatively recommend that the B factor be assigned a constant value of about 15 cm^{-1} for methyl–methyl radical pairs.

A number of additional issues must be considered when attempting to apply spin–orbit coupling theory to the interpretation of experimental rate constants for intersystem crossing (ISC). The geometry dependence of the other major ISC mechanism, hyperfine coupling (HFC), is very different from that for SOC. The local nature of the hyperfine interaction tends to render HFC nearly independent of geometry. Unless the two radical centers are very close together, e.g., nearest neighbors, each radical center makes its own independent contribution. It follows that HFC approaches a nonzero constant in the limit of large R.[7] The β proton HFC does depend on the torsional angle between the singly occupied orbital and the C–H bond,[20] but in flexible biradicals that angle is modulated much faster than the ISC rate constant, and the total HFC[21] assumes an average magnitude on the order of 0.01 cm^{-1}. This defines a natural boundary between "large" and "small" values of SOC. Large SOC (> ca. 0.1 cm^{-1}) is large enough to dominate ISC, while small SOC (< ca. 0.001 cm^{-1}) is negligible compared to HFC. Even when SOC is large, knowledge of SOC alone is not sufficient to predict ISC rate constant, k_{isc}. One must also know the regions of intersection of the singlet and triplet potential nergy surfaces,[16,22,23] and one must apply a dynamical theory, e.g., the Landau–Zener–Stueckleberg model.[24]

Most of our knowledge of k_{isc} in biradicals comes from nanosecond transient absorption measurements.[1,5,8,25] A trend which emerges from these studies applied to 3–6-membered biradicals is that k_{isc} increases as R decreases. It is reasonable to ascribe this to the R dependence of SOC, especially in view of recent results which show that SOC accounts for 75% of the ISC in a 1,12-biradical,[5b] 84% in a 1,11-biradical,[5b] and ca. 94% in a 1,8-biradical.[5c] Evidence has also been presented that, even in long biradicals, ISC is not efficient until the biradical adopts a conformation with small R.[5a] Experimentally, the decrease in SOC with increasing R is well established on a qualitative level.

Experimental evidence on the angular dependence of SOC is difficult to obtain. The vast majority of measurements of k_{isc} have been performed on flexible acyclic biradicals, for which a change in biradical conformation involves changes both in the angular orientation of the orbitals and in R. However, recent indirect measurements of k_{isc} via oxygen trapping of the triplet biradicals have been performed by Adam, Hannemann, and Wilson.[26] From Stern–Volmer slopes of the yields of oxygenated products, they estimated k_{isc} for **1** and **2** to be 1.05×10^7 s^{-1} and 1.1×10^6 s^{-1}, respectively.[26,27]

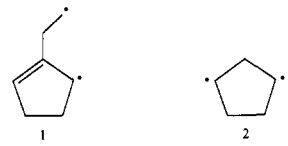

1 2

The value for **1** is typical of 1,4-biradicals,[1b,c] but the low value for **2** requires comment, especially since it is a 1,3-biradical with a smaller value of R. (Caldwell's recent study of 1,3-diaryltrimethylenes[25a] yields k_{isc} values of ca. 8×10^7.) The authors suggested that SOC in **2** is very small because of the parallel orientation of the orbitals in a time-averaged sense.[26b] This is a very appealing argument, but the authors also pointed out[26b] that ISC in triplet **2** is endothermic, since both experiment[28] and theory[16,22,29] agree in placing the triplet below the singlet. In order to undergo ISC the molecule must distort in an "envelope flapping" motion, essentially a disrotatory motion of the trimethylene moiety, until a singlet–triplet intersection is encountered. Figure 5 shows that SOC is large, SOC(50°,130°) = 0.6 cm^{-1} at the appropriate intersection in trimethylene, and the situation is probably qualitative the same in **2**. Because triplet **2** must move up in energy to reach the singlet–triplet intersection, ISC is associated with a Boltzmann factor. Buchwalter and Closs's experiment[28b] gave the value of 2.3 kcal/mol for the activation energy. Given Caldwell's measurement[25a] of 8×10^7 s^{-1} as the k_{isc} value for a freely rotating trimethylene in which singlet–triplet intersections encounter barriers no greater than RT,[30] application of the Boltzmann factor at the experimental temperature of 281 K predicts $k_{isc} = 1.3 \times 10^6$ s^{-1} for [2], within experimental error of the observed value. Thus the requirement to surmount a barrier accounts for the small value of k_{isc} in **2**.

Acknowledgment. We thank Professor Richard A. Caldwell for illuminating discussions. C.D. gratefully acknowledges National Science Foundation funding (NSF-84-21140).

(19) McWeeny, R. *J. Chem. Phys.* **1965**, *42*, 1717–1725.
(20) Kochi, J. *Adv. Free Radical Chem.* **1975**, *5*, 189–317.
(21) Total HFC is defined as the root mean square of all the hyperfine couplings.
(22) Goldberg, A. H.; Dougherty, D. A. *J. Am. Chem. Soc.* **1983**, *105*, 284–290.
(23) Doubleday, C., Jr.; McIver, J. W., Jr.; Page, M. *J. Am. Chem. Soc.* **1985**, *107*, 7904–7909.
(24) Eyring, H.; Walter, J.; Kimball, G. *Quantum Chemistry*; Wiley: New York, 1944; pp 326–330.
(25) (a) Mizuno, K.; Ichinose, N.; Otsuji, Y.; Caldwell, R. A. *J. Am. Chem. Soc.* **1985**, *107*, 5797–5798. (b) Caldwell, R. A.; Majima, T.; Pac, C. *Ibid.* **1982**, *104*, 629–630. (c) Freilich, S. F.; Peters, K. S. *Ibid.* **1981**, *103*, 6255–6257.
(26) (a) Adam, W.; Hannemann, K.; Wilson, R. M. *J. Am. Chem. Soc.* **1984**, *106*, 7646–7647. (b) Adam, W.; Hannemann, K.; Wilson, R. M. *Ibid.* **1986**, *108*, 929–935. (c) Adam, W.; Hannemann, K.; Wilson, R. M. *Angew. Chem., Int. Ed. Engl.* **1985**, *24*, 1071–1072.
(27) Other biradicals were also investigated, but the interpretation is less straightforward because little or no trapping occurred.
(28) (a) Buchwalter, S.; Closs, G. L. *J. Am. Chem. Soc.* **1975**, *97*, 3857–3858. (b) Buchwalter, S.; Closs, G. L. *Ibid.* **1979**, *101*, 4688–4694.
(29) Conrad, M.; Pitzer, R.; Schaefer, H. F., III *J. Am. Chem. Soc.* **1979**, *101*, 2245–2246.
(30) Yamaguchi, Y.; Schaefer, H. F., III *J. Am. Chem.* **1984**, *106*, 5115–5118.